The *in-situ* decoration of Ti_3C_2 quantum dots on Cu nanowires for high efficient electrocatalytic reduction of nitric oxide to ammonia

Baojing Li[a], Dongcai Shen[a], Zhengting Xiao[a,b], Quan Li[a], Shuo Yao[a], and Wentai Wang[a*]

[a] Key Laboratory of Marine Chemistry Theory and Technology, Ministry of Education; College of Chemistry and Chemical Engineering, Ocean University of China, Qingdao, 266100, China. Email: wentaiwang@ouc.edu.cn

[b] Key Laboratory of Biofuels, Qingdao Institute of Bioenergy and Bioprocess Technology, Chinese Academy of Sciences, Qingdao 266101, PR China

1. Determination of NH_3

The ammonia produced in the electrocatalytic NORR process was determined by UV-vis spectrophotometry with indophenol blue method. Specifically, 2 mL of solution after NORR test is added to 2 mL of 1.0 M NaOH solution (containing 5 wt% salicylic acid and 5 wt% sodium citrate), 1 mL of 0.05 M NaClO and 0.2 mL of 1 wt% $C_5FeN_6Na_2O$ are added, and the absorption spectrum of UV-vis tested after the solution was kept away from light for 2 hours in the greenhouse. The concentration of indophenol blue was measured at the wavelength of 655 nm in the absorption spectrum. The concentration absorption peak curve is calibrated with a series of standard NH_4Cl (aq) of different concentrations. The standard curve obtained by indophenol blue method is y=0.37131x+0.04886, R^2=0.9996, as shown in the figure.

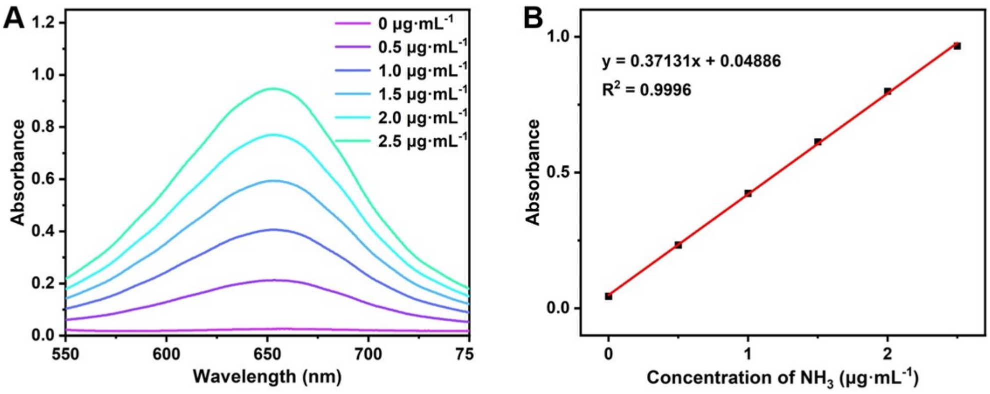

Fig. S1. (A) UV-vis absorption spectra of indole phenol determination at different concentrations of NH_4^+ at room temperature after 2 hours of avoiding light. (B) Calibration curve for estimating NH_4^+ concentration.

2. Determination of N_2H_4

N_2H_4 was determined by UV-vis using the method reported by Watt and Christp. Mix 0.599 g $C_9H_{11}NO$, 3 mL HCl and 30 mL C_2H_5OH as color developing agent for standby. Specifically, take 2 mL of experimental solution from the NORR electrolytic cell, add 2 mL of developer, mix it at room temperature for 15 minutes, and then conduct UV-vis analysis at 455 nm to test the absorbance of the obtained solution. Configure N_2H_4 measurement working curves with different concentrations to obtain the relationship between N_2H_4 with different concentrations and absorbance: y=0.77471x+0.02014, R^2=0.997.

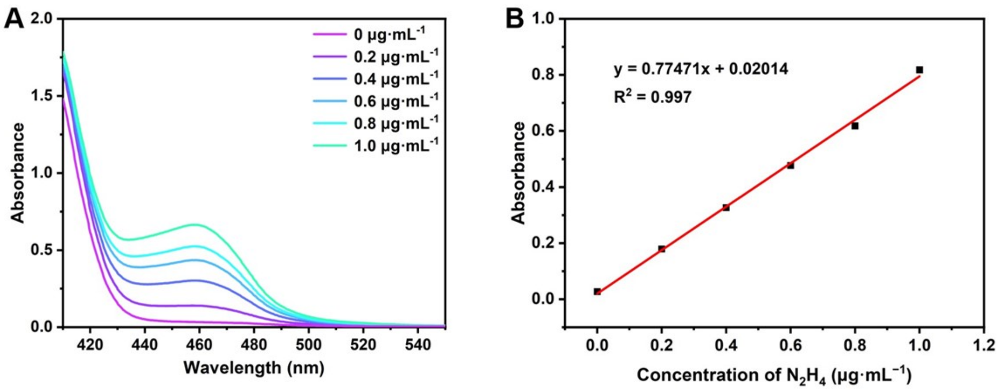

Fig. S2. (A) UV-vis absorption spectra measured after 20 minutes at different N_2H_4 concentrations at room temperature. (B) Calibration curve for estimating N_2H_4 concentration.

3. Determination of H_2

Determination of gas phase product H_2 by gas chromatography.

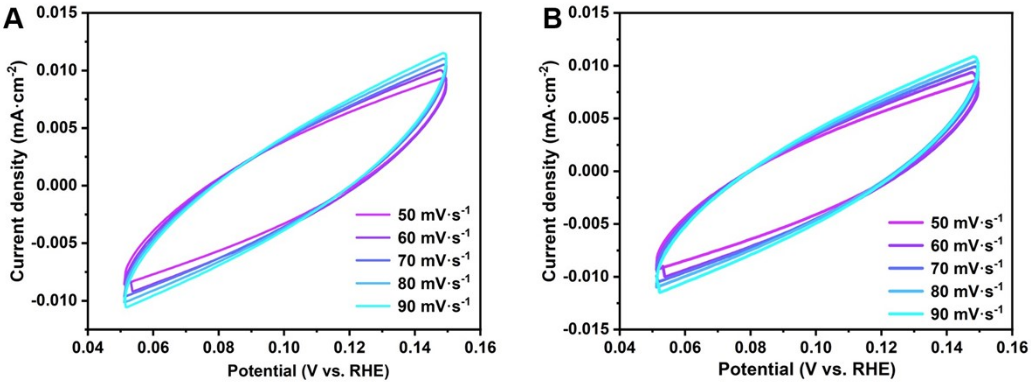

Fig. S3 The CV curves of (A) Cu NWs and (B) Ti_3C_2 QDs/Cu NWs at different scanning rates (50, 60, 70, 80, 90 mV/s).

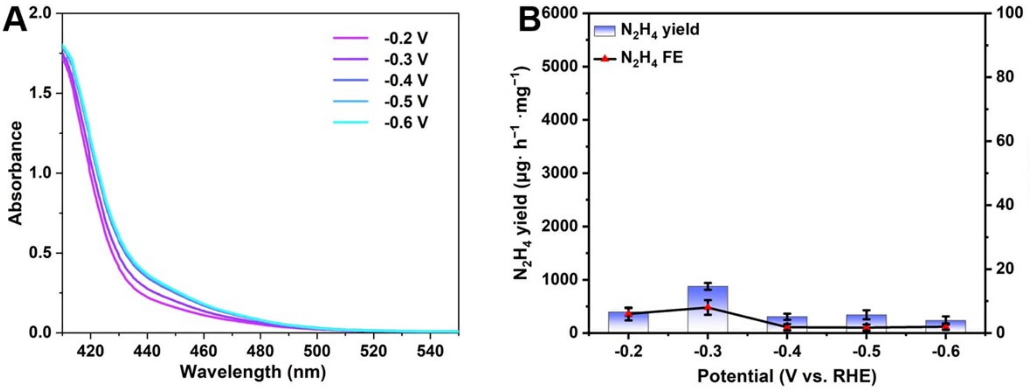

Fig. S4. The UV-vis absorption spectra of N_2H_4 were produced at Ti_3C_2 QDs/Cu NWs at different potentials.

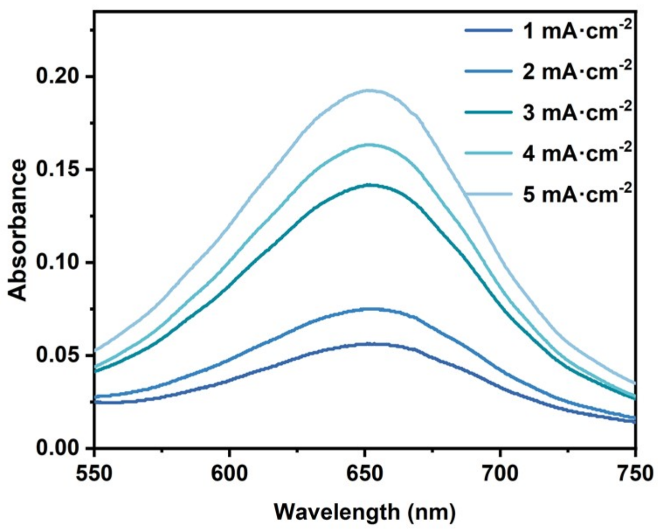

Fig. S5. UV-vis absorption spectra at different currents.

Table 1. Comparison of Ti_3C_2 QDs/Cu NWs and reported NORR performance

Catalyst	**Electrolyte**	**Potential (V vs. RHE)**	**NH_3 yield**	**FE (%)**	**Ref.**
Ti_3C_2 QDs/Cu NWs	0.1 M K_2SO_4	-0.4	5346.30 $\mu g \cdot h^{-1} \cdot mg^{-1}$	95.50	This work
Ni_2P/CP	0.1 M HCl	-0.2	33.47 $\mu mol \cdot h^{-1} \cdot cm^{-2}$	76.9	[1]
$Ru_{0.05}Cu_{0.95}$	0.5M Na_2SO_4	-0.49	17.68 $\mu mol \cdot cm^{-2} \cdot h^{-1}$	64.9	[2]
CoP/TM	0.2 M Na_2SO_4	-0.2	47.22 $\mu mol \cdot h^{-1} \cdot cm^{-2}$	88.3	[3]
FeP/CC	0.2 M PBS	-0.2	85.62 $\mu mol \cdot h^{-1} \cdot cm^{-2}$	88.49	[4]
Cu/P-TiO_2	0.1 M K_2SO_4	-0.3	3520.80 $\mu g \cdot h^{-1} \cdot mg^{-1}$	86.49	[5]
Cu-Ti hollow fiber	0.05M Na_2SO_4	-0.6	400 $\mu mol \cdot h^{-1} \cdot cm^{-2}$	90	[6]
NiNC@CF	0.5 M PBS	-0.5	94 $\mu mol \cdot h^{-1} \cdot cm^{-2}$	87	[7]
HCNF/CP	0.2 M Na_2SO_4	-0.6	22.35 $\mu mol \cdot h^{-1} \cdot cm^{-2}$	88.33	[8]
Ni@NC	0.1 M HCl	0.16	34.6 $\mu mol \cdot cm^{-2} \cdot h^{-1}$	72.3	[9]

NiO/TM	0.1 M Na_2SO_4+0.05 mM Fe^{2+}-EDTA	-0.6	2130 $\mu g \cdot h^{-1} \cdot cm^{-2}$	90	[10]
MoS_2/GF	0.1 M HCl + 0.5 mM Fe (II)SB	-0.7/0.1	99.6 $\mu mol \cdot cm^{-2} \cdot h^{-1}$	76.6	[11]
a-$B_{2.6}$C @ $TiO_{2/}$ Ti	0.1 M Na_2SO_4 + 0.5 mM Fe^{2+}-EDTA	-0.9	3678.6 $\mu g \cdot h^{-1} \cdot cm^{-2}$	87.6	[12]
Bi NDs/CP	0.1 M Na_2SO_4 + 0.05 mM Fe(II)EDT A	-0.50	1194 $\mu g \cdot h^{-1} \cdot mg^{-1}$	89.2	[13]
Bi@C	0.1 M Na_2SO_4 + 0.05 mM Fe(II)EDTA	-0.7/-0.4	1592.5 $\mu g \cdot h^{-1} \cdot mg^{-1}$	93	[14]
Ru-LCN	0.5 M Na_2SO_4	-0.2	45.02$\mu mol \cdot mg^{-1} \cdot h^{-1}$	65.96	[15]
Fe/C	0.5 M PBS	—	908$\mu mol \cdot cm^{-2} \cdot h^{-1}$	77	[16]

	0.5M H_2SO_4	—	1239μmol·cm^{-2}·h^{-1}	50.4	
MoC/NCS	0.1 M HCl	-0.8	1350±15μg·cm^{-2}·h^{-1}	89%±2 %	[17]

References

1. T. Mou, J. Liang, Z. Ma, L. Zhang, Y. Lin, T. Li, Q. Liu, Y. Luo, Y. Liu, S. Gao, H. Zhao, A. M. Asiri, D. Ma and X. Sun, High-efficiency electrohydrogenation of nitric oxide to ammonia on a Ni2P nanoarray under ambient conditions, *Journal of Materials Chemistry A*, 2021, **9**, 24268-24275.
2. J. Shi, C. Wang, R. Yang, F. Chen, N. Meng, Y. Yu and B. Zhang, Promoting nitric oxide electroreduction to ammonia over electron-rich Cu modulated by Ru doping, *Science China Chemistry*, 2021, **64**, 1493-1497.
3. J. Liang, W.-F. Hu, B. Song, T. Mou, L. Zhang, Y. Luo, Q. Liu, A. A. Alshehri, M. S. Hamdy, L.-M. Yang and X. Sun, Efficient nitric oxide electroreduction toward ambient ammonia synthesis catalyzed by a CoP nanoarray, *Inorganic Chemistry Frontiers*, 2022, **9**, 1366-1372.
4. J. Liang, Q. Zhou, T. Mou, H. Chen, L. Yue, Y. Luo, Q. Liu, M. S. Hamdy, A. A. Alshehri, F. Gong and X. Sun, FeP nanorod array: A high-efficiency catalyst for electroreduction of NO to NH3 under ambient conditions, *Nano Research*, 2022, **15**, 4008-4013.
5. L. Chen, W. Sun, Z. Xu, M. Hao, B. Li, X. Liu, J. Ma, L. Wang, C. Li and W. Wang, Ultrafine Cu nanoparticles decorated porous TiO2 for high-efficient electrocatalytic reduction of NO to synthesize NH3, *Ceramics International*, 2022, **48**, 21151-21161.
6. P. M. Krzywda, A. Paradelo Rodríguez, N. E. Benes, B. T. Mei and G. Mul, Effect of Electrolyte and Electrode Configuration on Cu-Catalyzed Nitric Oxide Reduction to Ammonia, *ChemElectroChem*, 2022, **9**, e202101273.
7. T. Muthusamy, S. Sethuram Markandaraj and S. Shanmugam, Nickel nanoparticles wrapped in N-doped carbon nanostructures for efficient electrochemical reduction of NO to NH3, *Journal of Materials Chemistry A*, 2022, **10**, 6470-6474.
8. L. Ouyang, Q. Zhou, J. Liang, L. Zhang, L. Yue, Z. Li, J. Li, Y. Luo, Q. Liu, N. Li, B. Tang, A. Ali Alshehri, F. Gong and X. Sun, High-efficiency NO electroreduction to NH3 over honeycomb carbon nanofiber at ambient conditions, *J Colloid Interface Sci*, 2022, **616**, 261-267.
9. S. Sethuram Markandaraj, T. Muthusamy and S. Shanmugam, Electrochemical Reduction of Nitric Oxide with 1.7% Solar-to-Ammonia Efficiency Over Nanostructured Core-Shell Catalyst at Low Overpotentials, *Advanced Science*, 2022, **9**.
10. P. Liu, J. Liang, J. Wang, L. Zhang, J. Li, L. Yue, Y. Ren, T. Li, Y. Luo, N. Li, B. Tang, Q. Liu, A. M. Asiri, Q. Kong and X. Sun, High-performance NH3 production via NO electroreduction over a NiO nanosheet array, *Chem Commun*, 2021, **57**, 13562-13565.

11. L. Zhang, J. Liang, Y. Wang, T. Mou, Y. Lin, L. Yue, T. Li, Q. Liu, Y. Luo, N. Li, B. Tang, Y. Liu, S. Gao, A. A. Alshehri, X. Guo, D. Ma and X. Sun, High-Performance Electrochemical NO Reduction into NH3 by MoS2 Nanosheet, *Angew Chem Int Ed Engl*, 2021, **60**, 25263-25268.
12. J. Liang, P. Liu, Q. Li, T. Li, L. Yue, Y. Luo, Q. Liu, N. Li, B. Tang, A. A. Alshehri, I. Shakir, P. O. Agboola, C. Sun and X. Sun, Amorphous Boron Carbide on Titanium Dioxide Nanobelt Arrays for High-Efficiency Electrocatalytic NO Reduction to NH3, *Angew Chem Int Ed Engl*, 2022, **61**, e202202087.
13. Y. Lin, J. Liang, H. Li, L. Zhang, T. Mou, T. Li, L. Yue, Y. Ji, Q. Liu, Y. Luo, N. Li, B. Tang, Q. Wu, M. S. Hamdy, D. Ma and X. Sun, Bi nanodendrites for highly efficient electrocatalytic NO reduction to NH3 at ambient conditions, *Materials Today Physics*, 2022, **22**, 100611.
14. Q. Liu, Y. Lin, L. Yue, J. Liang, L. Zhang, T. Li, Y. Luo, M. Liu, J. You, A. A. Alshehri, Q. Kong and X. Sun, Bi nanoparticles/carbon nanosheet composite: A high-efficiency electrocatalyst for NO reduction to NH3, *Nano Research*, 2022, **15**, 5032-5037.
15. Y. Li, C. Cheng, S. Han, Y. Huang, X. Du, B. Zhang and Y. Yu, Electrocatalytic Reduction of Low-Concentration Nitric Oxide into Ammonia over Ru Nanosheets, *ACS Energy Letters*, 2022, **7**, 1187-1194.
16. S. Cheon, W. J. Kim, D. Y. Kim, Y. Kwon and J.-I. Han, Electro-synthesis of Ammonia from Dilute Nitric Oxide on a Gas Diffusion Electrode, *ACS Energy Letters*, 2022, **7**, 958-965.
17. G. Meng, M. Jin, T. Wei, Q. Liu, S. Zhang, X. Peng, J. Luo and X. Liu, MoC nanocrystals confined in N-doped carbon nanosheets toward highly selective electrocatalytic nitric oxide reduction to ammonia, *Nano Research*, 2022, **15**, 8890-8896.